Proceedings of "Applications of Physics in Mechanical and Material Engineering" (APMME 2023)

UV-Filtration Properties of a Quasi-One-Dimensional Photonic Crystal

K.M. Gruszka* and M. Dośpiał

Department of Physics, Czestochowa University of Technology, Armii Krajowej Av. 19, 42-200 Częstochowa, Poland

Doi: 10.12693/APhysPolA.144.351 *e-mail: konrad.gruszka@pcz.pl

The paper presents a comprehensive investigation of the ultraviolet-filtration properties of a quasi-one-dimensional photonic crystal using the transfer matrix method. The photonic crystal structure forms a periodic stack that exhibits photonic suppression regions. By tailoring the layer thicknesses, we have designed a photonic crystal filter that selectively transmits ultraviolet light while efficiently suppressing unwanted wavelengths. Moreover, we demonstrate that a similar effect can be achieved by introducing an interlayer air gap, which, in turn, makes it possible to adjust the system during operation. Through rigorous simulations, the transmission characteristics of the proposed photonic crystal filter have been analyzed. The simulation results demonstrate that the filter exhibits a high degree of ultraviolet light transmission within a specific wavelength range, while effectively suppressing other wavelengths in the visible and near-infrared regions. The ability to selectively transmit ultraviolet light can be utilized in various fields, such as solar energy harvesting, ultraviolet photodetection, and optical sensing.

topics: matrix method, UV filters, tunable, electromagnetic (EM) propagation

1. Introduction

Tunable ultraviolet (UV) filters that allow for the transmission of specific UV light wavelengths are highly desired in various scientific applications due to their application versatility and precise control over the spectral range. The significance of such filters may be demonstrated when considering such fields as spectroscopy, photobiology and photomedicine, optoelectronics and nanotechnology, solar research, or photovoltaics, which remains a very active research area nowadays. For example, in spectroscopy, the ability to transmit specific wavelengths of UV allows the study of the unique spectral signatures of different compounds, which in turn enables the identification, quantification, and analysis of substances in fields such as chemistry, biochemistry, and environmental science [1–3]. In the field of photobiology, the effects of UV radiation on living organisms are studied because different wavelengths of UV light have varying biological impacts, ranging from DNA damage to influence on cellular processes. Tunable UV filters facilitate precise manipulation of the UV spectrum incident on biological samples, enabling researchers to investigate the specific effects of different wavelengths on cellular mechanisms, photoreceptors, and photosensitive molecules [4]. In photomedicine, tunable UV filters are crucial for selecting the most appropriate wavelengths for therapeutic applications, such as targeted photodynamic therapy or UV-induced sterilization [5]. In optoelectronic and nanotechnology, certain semiconductor materials, such as gallium nitride (GaN), are widely used in UV LEDs and UV detectors [6]. Tunable filters allow researchers to optimize the transmission characteristics of these devices, enhancing their efficiency, sensitivity, and performance. Additionally, in nanofabrication processes, tunable UV filters are utilized for precise control of the UV exposure, enabling the patterning and structuring of nanoscale features on substrates [7, 8]. As for solar research and photovoltaics, the study of solar radiation and its interaction with the Earth's atmosphere is essential for understanding climate dynamics, atmospheric chemistry, and solar energy conversion [9]. Different UV wavelengths have distinct effects on the Earth's energy budget, ozone layer, and photochemical reactions. Tunable UV filters help scientists isolate and investigate specific UV bands, allowing them to gain insights into the detailed mechanisms of these processes and accurately quantify their impact on climate change and environmental systems.

The above examples are only a small part of the various applications faced by this type of devices, however, these examples clearly show that the demand for this type of solutions not only does not decrease, but also promises further increased exploration of photonics and its future applications, simply leading to advancements in various scientific disciplines and technological applications [10].

Quasi-one-dimensional photonic crystals (PCs) have emerged as a fascinating area of research in the field of photonics due to their unique optical properties and potential applications. These structures consist of alternating layers or periodic arrays of materials with different refractive indices, which leads to the formation of bandgaps and selective reflection or transmission of specific wavelengths of light. In recent years, there has been growing interest in utilizing quasi-one-dimensional photonic crystals for the fabrication of tunable UV filter devices, enabling precise control over the transmission of ultraviolet (UV) light. The design and analysis of such devices often rely on computer simulations based on the transfer matrix method (TMM) [11], which is well-suited for investigating the optical properties of these complex structures [12]. In this paper, we present a comprehensive study on the design, simulation, and characterization of tunable UV filters based on quasi-one-dimensional photonic crystals, employing the transfer matrix method as a powerful tool for analyzing their optical behavior. By exploring the tunability of these filters, we aim to contribute to the development of advanced UV filtering technologies with applications in spectroscopy, photomedicine, optoelectronics, and beyond.

2. Computational methods

The TMMs method governing equation [13, 14]

$$\begin{bmatrix} E_{in}^{(+)} \\ E_{in}^{(-)} \end{bmatrix} = \Gamma \begin{bmatrix} E_{out}^{(+)} \\ E_{out}^{(-)} \end{bmatrix} \tag{1}$$

describes incident wave $E_{in}^{(+)}$ incident on the boundary of the mediums, $E_{in}^{(-)}$ is reflected wave propagating in an antiparallel direction, $E_{out}^{(+)}$ is wave coming out of the system, while characteristic matrix Γ is defined as

$$D_{in,j}\Big(\prod_{j=1}^{J} P_j D_{j,j+1}\Big) = \begin{bmatrix} \Gamma_{11} & \Gamma_{12} \\ \Gamma_{21} & \Gamma_{22} \end{bmatrix} \tag{2}$$

and

$$P_j = \begin{bmatrix} \mathrm{e}^{\mathrm{i}\varphi_j} & 0 \\ 0 & \mathrm{e}^{-\mathrm{i}\varphi_j} \end{bmatrix}, \tag{3}$$

$$\varphi_j = d_j n_j \frac{2\pi}{\lambda} \cos(\phi_j), \tag{4}$$

where d_j is j-th layer thickness, n_j — j-th layer refractive index, λ — incident wavelength, and ϕ_j — j-th layer incidence angle.

The last one, $D_{j,j+1}$, called the transmittance matrix is defined as

$$D_{j,j+1} = \frac{1}{t_{j,j+1}} \begin{bmatrix} 1 & r_{j,j+1} \\ r_{j,j+1} & 1 \end{bmatrix}, \tag{5}$$

where the symbols $t_{j,j+1}$ and $r_{j,j+1}$ denote the Fresnel reflectance and transmittance coefficients of the electromagnetic wave at the transition from medium j to medium $j+1$, assuming that the wave propagates towards the positive values of the X axis of the multilayer system (parallel to normal vector of the system layers, while these layers are parallelograms). The schematic illustration of the studied system is presented in Fig. 1. The system consists of 7 layers made using two materials, namely fused silica and Vitron IG, and their refractive indexes are $n_A = 1.4570$ and $n_B = 2.5385$, respectively. When the air gap was used, the refractive index was set to $n_X = 1.0$. Whenever an air gap was introduced into the system, it was placed after layer 3 (see Fig. 1). Simulation takes into account the extinction coefficients of these materials, which are 4.4788×10^{-7} for Vitron. In the case of fused silica and air gap, their corresponding extinction coefficients are $k = 0$.

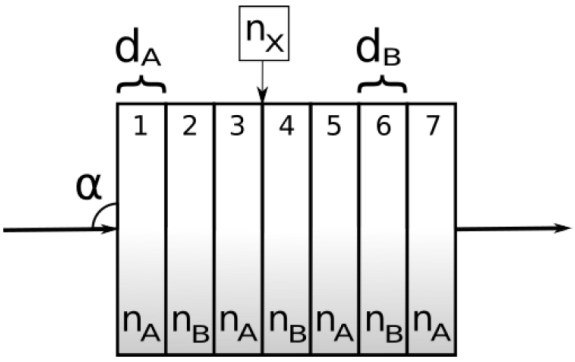

Fig. 1. Schematic diagram of waveguide with variable hole-defects. The spacing between hole centers is always fixed to 2 μm on both sides of the defect. For ease of readability, we present only selected defect sizes.

3. Results and discussion

The first quasi-one-dimensional photonic crystal was prepared to be centro-symmetric with a symmetry axis located at layer 4. The thickness of A material, d_A, was fixed to 15 nm, while the thickness of layer B, d_B, was systematically reduced from 20 down to 11 nm in a 1 nm step. The topology of the system was binary, implementing $\{A, B, A, B, A, B, A\}$ structure. Figure 2 shows the transmission spectra for this photonic crystal. As can be seen, for each case the single transmission spectrum consists of one sharp peak with a transmittance maximum at 100% (all transmittance spectra and maps are normalized to 1, where 1 corresponds to 100%) and a long "tail" with nearly 47% average transmission for the case when $d_X = 11$ nm and 67% when $d_X = 20$ nm. Reducing the thickness of the layer d_B leads to a twofold behavior of the overall transmission. Firstly, it is visible that the transmission maximum shifts towards shorter wavelengths, while not only maintaining the

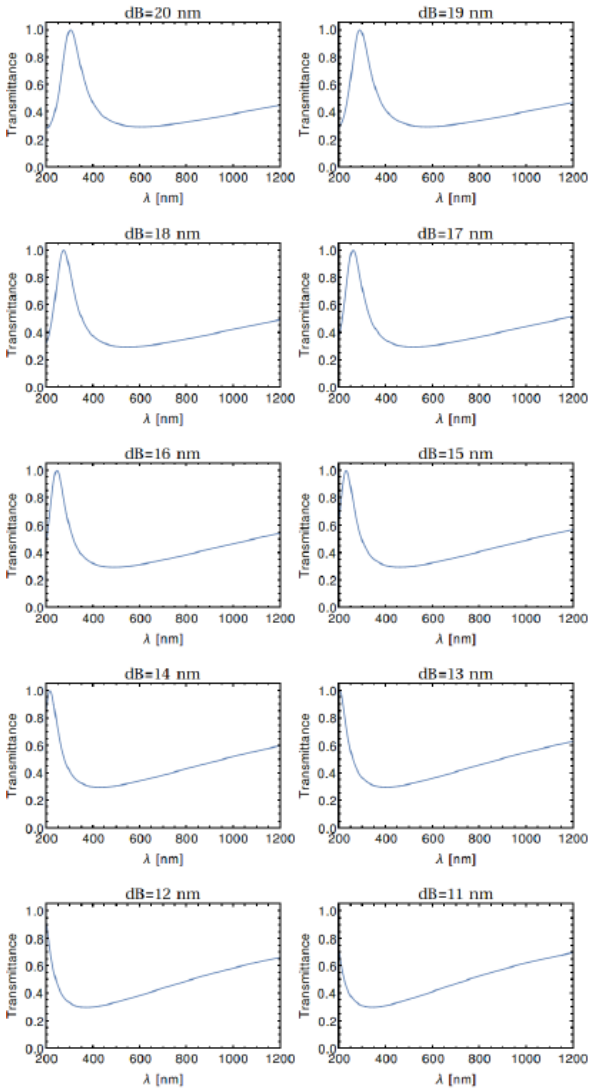

Fig. 2. Transmittance in function of incident wavelength at incident angle $\theta = \pi/4$. The B layer thickness (Vitron) was systematically decreased, as denoted.

transmittance maximum but also conserving the transmission peak shape. A narrow half-width of the transmittance peak is desirable as it limits the range of wavelengths passing through the system. Secondly, the transmittance from the infrared wavelength side (above 800 nm) increases, which is undesirable in this case. It should be noted, however, that the high transmittance at the peak of the maximum, due to the fact that it reaches as much as 100% in this place, allows for assembling several filters in a cascade, one after the other, assuming that the distance between the filters is sufficiently large (i.e., much greater than the desired wavelength of the transmitted UV light). Maintaining such a large gap (e.g., 10 μm or more) will limit the interaction between the filters to a minimum and will allow for undisturbed operation as if it were single.

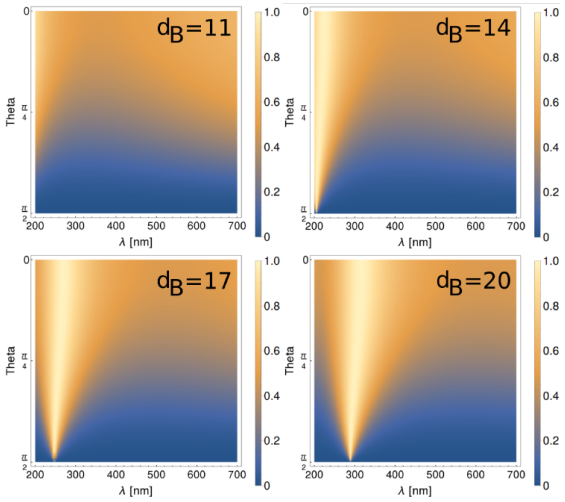

Fig. 3. Transmittance maps for the structure without air gap; d_B is the layer B thickness. The θ angle is the angle of incidence measured to the layer normal, and brightness is the transmittance.

Figure 3 shows in the form of transmission maps the behavior of the system when the angle of incidence α of light is changed in the range from 0 to 90° (0 to $\pi/2$). As can be seen, the selectivity of the filter increases as the incident wave tends to $\theta = \pi/2$ (please note that θ is defined with respect to the normal of the layer). The usable range for this photonic structure seems to lay between $\pi/4$ and $pi/2$; below this angle, the filter starts to transmit significant amounts of electromagnetic waves over a wide range of wavelengths.

Next, we introduced a variable air gap between layers number 3 and 4 (for reference, see Fig. 1). The presence of an air gap is very desirable because it basically allows one to modify the parameters of the filter without having to manufacture new photonic crystal, as it was a necessity in the first photonic crystal (PC) case. Unfortunately, the introduction of such an air gap may introduce potentially undesirable properties and deteriorate the filtering properties of the system. Air, on the other hand, does not strongly block UV radiation and allows modifications to the geometry of the PC structure to be made relatively easily. The introduction of the air gap required additional fine-tuning of the rest of the PC layers and a decrease in layer A thickness to $d_A = 13$ nm. Figure 4 shows the transmittance of the air gap photonic crystal, depending on the decreasing thickness of the air layer. As can be seen, the shape of the transmittance curve is similar in character to the first PC (without an air gap). In this case, a single peak can also be observed, although its transmittance at the peak of the maximum is lower and amounts to 89% for the structure in which the thickness of the air layer is $d_X = 30$ nm, but increases to 99% for $d_X = 3$ nm. The half-width of the peak has

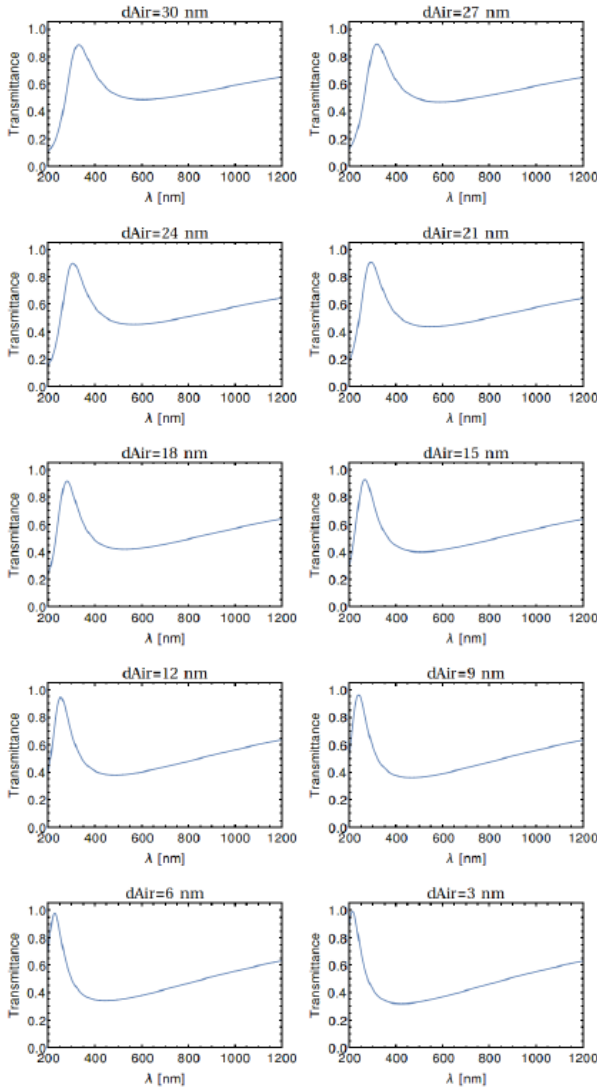

Fig. 4. Transmittance in function of incident wavelength at incident angle $\theta = \pi/4$ for the system with air gap. The gap size (d_{Air}) was systematically reduced, as denoted.

also increased, which, as mentioned earlier, negatively affects the selectivity of the filter. As in the first case, reducing the thickness of this layer shifts the transmittance peak towards lower wavelengths of electromagnetic radiation, while increasing the transmittance in the infrared region.

The transmittance maps presented in Fig. 5 are also of a similar nature as in the case of the first studied structure. Their in-depth analysis shows that this time the filter usability range (understood as the possibly narrow transmittance peak and the smallest possible transmittance for infrared light) is narrower than in the case of a structure without an air gap. This range can be extended by using a narrower air gap, but this involves shifting the transmittance maximum towards the light from the infrared range.

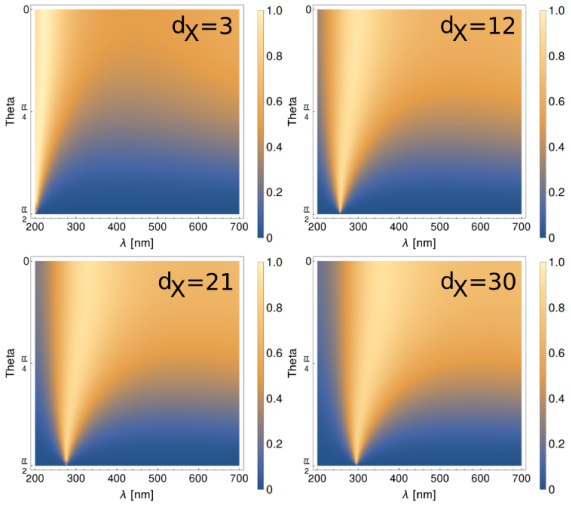

Fig. 5. Transmittance maps for the structure with air gap; d_X is the air gap thickness. The θ angle is the angle of incidence measured to the layer normal, and brightness is the transmittance.

4. Conclusions

The investigation into the UV-filtration properties of a quasi-one-dimensional photonic crystal has yielded valuable insights into the performance of the studied photonic structure. Through comprehensive analysis, several crucial findings have emerged. The transmittance spectra exhibit a distinctive behavior characterized by a sharp transmission peak with a transmittance maximum of 100%, accompanied by an extended "tail" exhibiting average transmissions of approximately 47% and 67% for respective thicknesses of $d_X = 11$ nm and $d_X = 20$ nm. The manipulation of the layer thickness d_B revealed intriguing outcomes, resulting in a dual effect on overall transmission. Firstly, a shift of the transmission peak towards shorter wavelengths was observed, while maintaining its shape and maximizing transmittance. The subsequent increase in transmittance at longer wavelengths was noted, albeit being undesirable. The filter's optimal operational range was found between $\pi/4$ and $\pi/2$; deviating beyond this range resulted in broader transmission of electromagnetic waves. The introduction of a variable air gap allowed for real-time parameter adjustments. Considering the air gap configuration, the transmittance curves maintained a single-peak nature, albeit with peak transmittance values decreasing to 89% for $d_X = 30$ nm and increasing to 99% for $d_X = 3$ nm. This led to a wider peak half-width, diminishing filter selectivity. Transmittance maps paralleled those of the initial structure, revealing a narrower usability range due to the air gap, and although this range could expand with a smaller air gap, it shifted the transmittance peak towards infrared light.

In summary, our study unveils the intricate interplay of layer parameters, incident angles, and air gap presence in influencing UV-filtration properties of quasi-one-dimensional photonic crystals. These findings offer practical design insights for optimizing photonic filters for UV applications, prompting further exploration and refinement of such systems.

Acknowledgments

This research was supported in part by PLGrid Infrastructure.

References

[1] Y. Zhang, S. Wu, P. Sun, *Sci. Total Environ.* **899**, 165702 (2023).

[2] S. Arsenault-Escobar, J.F. Fuentes-Galvez, C. Orellana, S. Bollo, P. Sierra-Rosales, S. Miranda-Rojas, *Spectrochim. Acta A* **292**, 122400 (2023).

[3] K. Gruszka, *Acta Phys. Pol. A* **139**, 617 (2021).

[4] K. Prabakaran, H. Oh, R. Manivannan, S. Hyeong Park, Y.-A Son, *Spectrochim. Acta A* **279**, 121437 (2022).

[5] C. Ruiz-Díez, M. Navarro-Segarra, R. Barrena, T. Gea, J.P. Esquivel, *Environ. Technol. Innov.* **31**, 103199 (2023).

[6] W. Ding, X. Meng, *J. Alloys Compd.* **866**, 157564 (2021).

[7] J. Yan, X. Fan, Y. Liu, K. Qu, Y. Yu, R.-Z. Li, *Appl. Mater. Today* **32**, 101840 (2023).

[8] J.H. Lee, D.H. Kim, J. Won, D.W. Lee, J.Y. Oh, Y. Liu, Y.-P. Park, H.-C. Jeong, D.-S. Seo, *Mater. Chem. Phys.* **269**, 124771 (2021).

[9] F. Yíldrim, Z. Orhan, Ş. Aydoğan, *Mater. Res. Bull.* **159**, 112113 (2023).

[10] K.M. Gruszka, M. Dośpiał, *Acta Phys. Pol. A* **142**, 101 (2022).

[11] M. Asif, A. Afaq, M. Amin, K. Raouf, A. Majeed, M. Asif, *Mater. Today Commun.* **37**, 106966 (2023).

[12] S. Garus, J. Garus, M. Szota, M. Nabiałek, K. Gruszka, K. Błoch, *Arch. Mater. Sci. Eng.* **64**, 110 (2013).

[13] T.G. Mackay, A. Lakhtakia, *The Transfer Matrix Method in Electromagnetics and Optics*, Springer International Publishing, 2020.

[14] M. Born, E. Wolf, A.B. Bhatia, P.C. Clemmow, D. Gabor, A.R. Stokes, A.M. Taylor, P.A. Wayman, W.L. Wilcock, *Principles of Optics: Electromagnetic Theory of Propagation, Interference and Diffraction of Light*, 7th ed., Cambridge University Press, 1999.